Zootaxa 1938: 40–60 (2008)
www.mapress.com/zootaxa/

ISSN 1175-5326 (print edition)
ZOOTAXA
ISSN 1175-5334 (online edition)

Larval anatomy of Andean tadpoles of *Telmatobius* (Anura: Ceratophryidae) from Northwestern Argentina

M. FLORENCIA VERA CANDIOTI

CONICET. Instituto de Herpetología, Fundación Miguel Lillo. Miguel Lillo 251 (4000) Tucumán, Argentina.
E-mail: florivc@yahoo.com

Abstract

In this paper I study the oral, buccopharyngeal, and musculoskeletal configuration in tadpoles of nine *Telmatobius* species from Northwestern Argentina (*T. atacamensis*, *T. ceiorum*, *T. laticeps*, *T. oxycephalus*, *T. pinguiculus*, *T. pisanoi*, *T.* cf. *schreiteri*, *T. scrocchii*, and *T. stephani*; N = 30, Gosner stages 31–36). Specimens were prepared according to standard clearing and staining protocols; additionally, I applied landmark and outline-based geometric morphometric methods in order to quantify shape variation in chondrocrania, hyobranchial skeletons, and suprarostral cartilages. Although preliminary, results show a marked morphological uniformity on the analyzed levels, and overlapping interspecific and intraspecific variation, which renders species discrimination difficult. Some distinctive traits for the genus are bicuspidate buccal spurs, peculiar arrangement of buccal roof and floor papillae, tetrapartite suprarostral, adrostral cartilages, a lateral slip of the m. subarcualis rectus II-IV invading branchial septum IV, and a characteristic pattern of muscles inserted on the diaphragm. The conservative larval internal morphology in this genus could be explained by a recent speciation and a development possibly characterized by the postmetamorphic appearance of specific features.

Resumen

En este trabajo estudio la morfología oral, bucofaríngea y musculoesquelética de larvas de nueve especies de *Telmatobius* del Noroeste argentino (*T. atacamensis*, *T. ceiorum*, *T. laticeps*, *T. oxycephalus*, *T. pinguiculus*, *T. pisanoi*, *T.* cf. *schreiteri*, T. *scrocchii* y *T. stephani*; N = 30, estadios de Gosner 31–36). Los especímenes se prepararon siguiendo protocolos clásicos de transparentación y coloración diferencial; adicionalmente, apliqué métodos de morfometría geométrica basada en landmarks y contornos para cuantificar la variación de formas en condrocráneos, esqueletos hiobranquiales y cartílagos suprarostrales. Aunque de carácter preliminar, los resultados muestran una notable uniformidad morfológica en los niveles analizados, y una variación intraespecífica que se superpone con la interespecífica, dificultando la distinción entre especies. Algunos rasgos distintivos del género son un par de espolones bucales bífidos, un arreglo particular de las papilas del techo y piso bucales, suprarostral tetrapartito, adrostrales, un haz del m. subarcualis rectus II-IV invadiendo el septo branquial IV, y un patrón aparentemente característico de los músculos insertos en el diafragma. La morfología larval interna conservadora en el género podría explicarse por una especiación reciente y un desarrollo posiblemente caracterizado por la aparición postmetamórfica de los rasgos específicos.

Key words: *Telmatobius*, tadpoles, buccal cavity, musculoskeletal configuration, geometric morphometrics

Introduction

The genus *Telmatobius* (Ceratophryidae: Telmatobiinae) includes 57 species of Andean frogs distributed from Southern Ecuador to Northern Chile and Northwestern Argentina (Frost *et al.* 2006, updated in Frost 2008); till moment, 14 species are cited for Argentina (Lavilla & Barrionuevo 2005). The literature on the genus

 Accepted by M. Vences: 22 Oct. 2008; published: 21 Nov. 2008

comprehends mainly studies on adult specimens, considering external morphology, morphometrics, osteology, soft anatomy, genetics, reproductive and ecological aspects, etc. (e.g., Vellard 1946; 1960; Pisanó 1954/1957; Laurent 1970; 1973; 1977; 1979; Lynch 1971; 1978; Heyer 1975; Trueb 1979; Cei 1980; 1986; Lavilla & Laurent 1988a,b; Montero & Pisanó 1990; Wiens 1993; Córdova & Descailleaux 2005; Sinsch *et al*. 2005; see a commented bibliographic list in Lavilla 2005). Phylogenetic relationships within the genus have not been completely elucidated, and the most recent approaches are the researches by Aguilar (2006) and Barrionuevo (in prep.), on Peruvian and Argentinean species respectively.

As regard to tadpoles, most of the available literature concerns external morphological features (e.g., Pisanó & Rengel 1954; Trueb 1979; Lavilla 1983; 1984; 1985; Díaz & Valencia 1985; Lavilla & Scrocchi 1986; Lavilla & De la Riva 1993; Cuevas & Formas 2002; De la Riva & Harvey 2003; Formas *et al*. 2003, 2006; De la Riva 2005; Formas *et al.* 2005; Lehr 2005; Merino-Viteri *et al.* 2005). Wassersug and Heyer (1988), Carr and Altig (1991), Fabrezi and Lavilla (1993), Lavilla and De la Riva (1993), Palavecino (1999), Aguilar and Pacheco (2005), Aguilar (2006), Aguilar *et al*. (2007) and Vera Candioti (2007) contributed with punctual descriptions and comparative studies on skeletal, muscular and buccopharyngeal configuration.

The aims of this paper are (1) to analyze oral, buccopharyngeal, and musculoskeletal features of tadpoles of nine species of *Telmatobius* from Northwestern Argentina, and (2) to discuss this in a more general frame of larval morphology associated with phylogenetic and ecological aspects; this intend to provide base data that can be useful for more integrative studies on anuran tadpoles.

Material and Methods

I worked with tadpoles housed at the Herpetological Collection of the Instituto de Herpetología, (Fundación-Miguel Lillo; N = 30, Gosner–1960–stages 31–36), collected from varied sites in Northwestern Argentina. Studied species are: *Telmatobius atacamensis*, *T. ceiorum*, *T. laticeps*, *T. oxycephalus*, *T. pinguiculus*, *T. pisanoi*, *T.* cf. *schreiteri*, *T. scrocchii*, and *T. stephani*; specimen list and collection data are detailed in Table 1. For oral and buccopharyngeal configuration studies, I exposed buccal roof and floor, staining structures with methylene blue prior to observation. For skeleton and musculature studies, specimens were treated with a double staining protocol (Wassersug 1976a), interrupting the procedure before clearing, and then staining with lugol solution to enhance the contrast between skeleton and muscles. The terminology employed to describe oral, buccal, and musculoskeletal structures is that suggested by Altig (2007), Wassersug (1976b), and Haas (2003) respectively.

In order to explore skeletal interspecific variation, I carried out preliminary analyses on shape variation of three structures through geometric morphometrics (N = 1–5 per species). For the study of chondrocranium and hyobranchial skeleton shape, on the right side of cartilage pictures I defined 28 and 24 landmarks respectively, and I applied a principal component analysis on shape variable matrices (partial warps + uniform component), first separately and then combined (details on landmark-based geometric morphometrics in Rohlf & Bookstein 1990, Monteiro & Furtado dos Reis 1999, and Zelditch *et al.* 2004, among others; landmark selection based on Vera Candioti *et al.* 2007). For suprarostral cartilages, I applied the mean-centered approach of extended eigenshape analysis –EEA–, which describes curves through a *phi* function that represents the deviation from a circumference (closed curves in this case), plus landmarks delimiting comparable segments, also calculating a minimum number of points to describe each segment (details on standard and extended eigenshape analysis in Lohmann 1983; MacLeod 1999; Krieger *et al*. 2007, among others). For certain structures, this method gives more accurate results than the elliptic Fourier analysis –EFA– (Kuhl & Giardina 1982), since additional landmarks constrain the alignment of outlines to comparable segments, and then "the extraneous variation generated through biological miscorrespondence of the outline can be reduced" (MacLeod 1999).

TABLE 1. Studied specimens and collection data.

	Collection number	Collection site	Gosner stages
Telmatobius atacamensis	FML04472*	San Antonio de los Cobres, Salta	34, 36, 36
Telmatobius ceiorum	FML05068	Tafí del Valle, Tucumán	35, 36
	FML05070	Tafí del Valle, Tucumán	36
	FML05074	Tafí del Valle, Tucumán	31
	FML05075	Tafí del Valle, Tucumán	31
Telmatobius laticeps	FML04625	Tafí del Valle, Tucumán	31, 31, 32
Telmatobius oxycephalus	FML10211	Parque Nacional Calilegua, Jujuy	31, 34
Telmatobius pinguiculus	FML05536	La Ciénaga, Catamarca	32
Telmatobius pisanoi	FML04081	Tafí del Valle, Tucumán	36
	FML04613	Tafí del Valle, Tucumán	31, 36, 36
	FML04609	Tafí del Valle, Tucumán	31
Telmatobius cf. *schreiteri*	FML05113	El Plumerito, La Rioja	31, 31
	FML05161	Macho Muerto, La Rioja	31, 36
Telmatobius scrocchii	FML04482	Río el Arenal, Catamarca	31, 31, 32, 31, 34
Telmatobius stephani	FML05534	La Cumbrecita, Catamarca	31, 34, 35

*Tadpoles of this lot were used for external morphology examination; all larvae of a new lot, collectioned at the same locality, were employed for dissection and thus no whole specimens were deposited at the Herpetological Collection.

Results

I describe oral, buccal, and musculoskeletal configuration of nine *Telmatobius* species studied. Variable features are detailed for corresponding species, when relevant.

Oral apparatus and buccopharyngeal cavity. The oral disc represents about 23–25% of the tadpole body length. It is oblong and not emarginated; in relaxed position, the lower labium often forms two ventrolateral folds. It is lined by a single row of conical marginal papillae, interrupted by a dorsal gap that occupies almost half of the upper labium. Large submarginal papillae appear in several series in the commissural region, and aligned in one row in the lower labium. Labial teeth form frequently on lower submarginal papillae. Rostrodonts are curve, well-developed, keratinized, dark, and serrated. Labial tooth rows have similar length, and are disposed according to a 2(2)/3(1) labial tooth row formula (Fig. 1). Labial teeth have an oblong, curve head with 10–14 cusps, a short, poorly defined body, and a wide sheath. In *Telmatobius oxycephalus*, *T. scrocchii*, and *T. stephani*, the head curvature is less marked than in the remaining species (Fig. 2).

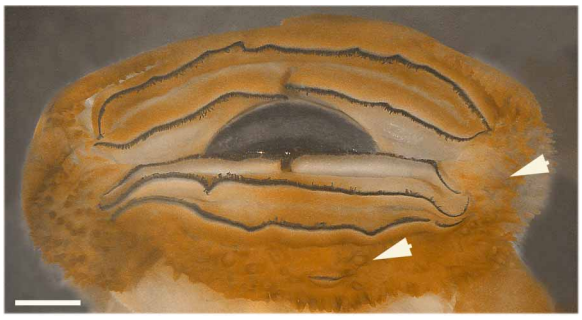

FIGURE 1. Oral apparatus in *Telmatobius*. *T. ceiorum*, frontal view. The arrows show commissural and lower labium submarginal papillae. Scale line = 1 mm.

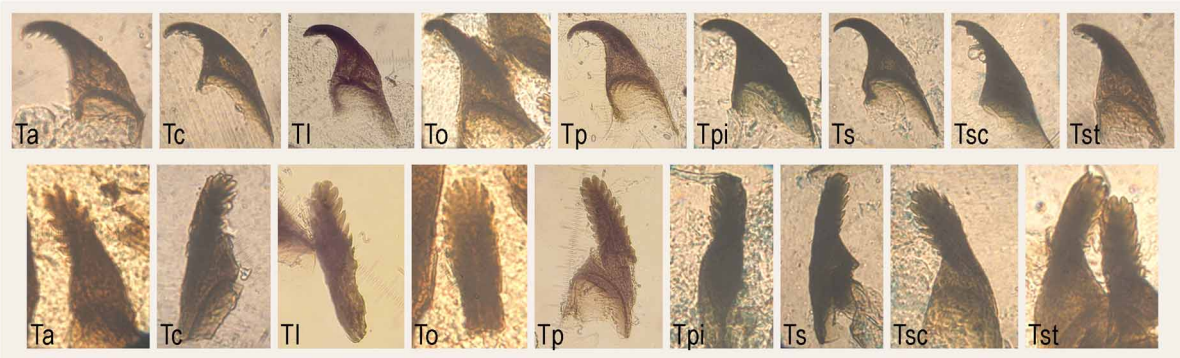

FIGURE 2. Labial teeth in *Telmatobius* (tooth row A1). Lateral (top) and frontal (bottom) views; Ta *T. atacamensis*, Tc *T. ceiorum*, Tl *T. laticeps*, To *T. oxycephalus*, Tp *T. pinguiculus*, Tpi *T. pisanoi*, Ts *T.* cf. *schreiteri*, Tsc *T. scrocchii*, Tst *T. stephani*. Magnification = 1000x, excepting *T. laticeps* and *T. pinguiculus*, with magnification = 400x.

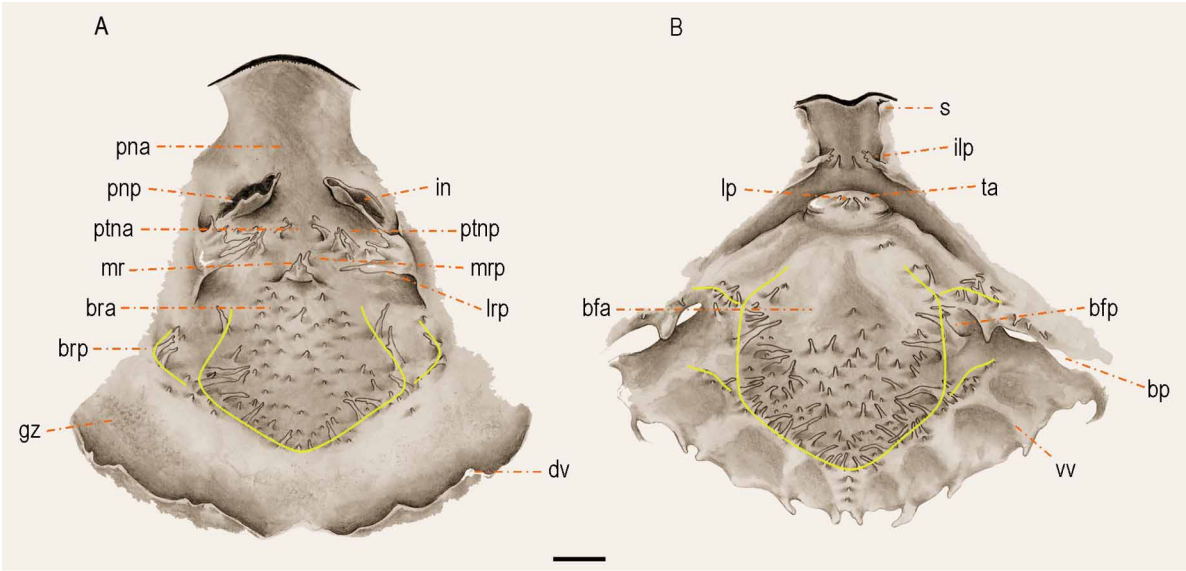

FIGURE 3. *Telmatobius atacamensis* buccal cavity, stage 36. (A) Buccal roof, (B) Buccal floor. bfa buccal floor arena, bfp buccal floor papilla, bp buccal pocket, bra buccal roof arena, brp buccal roof papilla, dv dorsal velum, gz glandular zone, ilp infralabial papilla, in internal nare, lp lingual papilla, lrp lateral ridge papilla, mr median ridge, mrp median ridge papilla, pna prenarial arena, pnp prenarial papilla, ptna postnarial arena, ptnp postnarial papilla, s spur, ta tongue anlage, vv ventral velum. Yellow lines show the two (roof) and three (floor) papilla arrangements. Scale line = 1 mm.

The buccal roof (Figs. 3 and 4) is rhomboidal and unpigmented. The prenarial arena is naked, or shows scarce pustules. The internal nares are oblong, arranged at an angle of 31–48º regarding the transversal axis; the extreme values correspond to *Telmatobius pinguiculus* and *T.* cf. *schreiteri*, respectively; 1–3 small prenarial papillae may appear on the anterior margin, and the nasal valve is poorly developed. On the postnarial arena, 3–4 pairs of tall, conical papillae align in an inverted V pattern, accompanied by several pustules and low papillae; papillae of the second pair are taller than the others. Lateral ridge papillae are flat, wide, well-developed, with 3–5 uneven, frequently pustulate tips. The median ridge is disposed at the level of lateral ridge papillae; it is triangular, with a markedly uneven margin, and in its folded position, conceals a couple of small pustules or low papillae anteriorly placed. The buccal roof arena is ovoid and limited by 7–12 pairs of symmetrically arranged marginal buccal roof arena papillae; these papillae are tall, conical and pustulate, the anterior pair more developed; numerous pustules and low papillae appear among the main papillae; on the arena central region, posterior to the median ridge, several pustules and small papillae are scattered. A second papilla arrangement includes conical papillae disposed following a line that continues the arena posterior

edge, diverging lateral and anteriorly, and often ending in discrete groups of 3–6 simple papillae. Posteriorly, the wide glandular region appears in an open-V pattern, and includes conspicuous, large secretory pits. The dorsal velum is short and recurved, and interrupts medially in a wide gap.

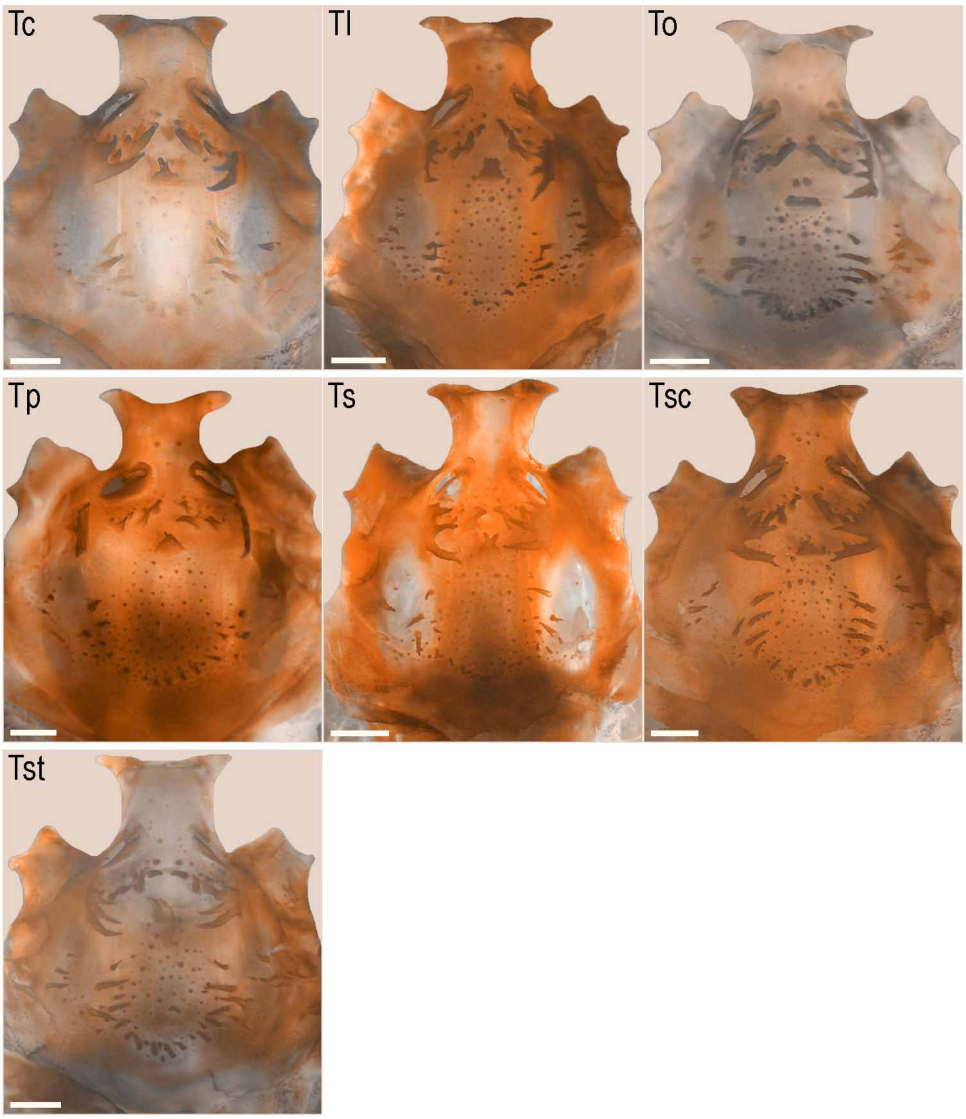

FIGURE 4. Buccal roofs in other *Telmatobius*. Tc *T. ceiorum*, Tl *T. laticeps*, To *T. oxycephalus*, Tp *T. pinguiculus*, Ts *T.* cf. *schreiteri*, Tsc *T. scrocchii*, Tst *T. stephani*. *T. pisanoi* picture is not shown because after examination the specimen was too destroyed to be photographed. Scale lines = 1 mm.

The buccal floor (Figs. 3 and 5) also lacks pigmentation. Posteriorly to the infrarostrodonts, a couple of small, keratinized, scarcely prominent, and bicuspidate spurs appear, medially oriented. Two pairs of infralabial papillae place posteriorly; the medial ones are small and conical, and the lateral ones, directed medially from the medial edge of the Meckel's cartilage, are larger, flat, slightly pustulate, and do not overlap in the middle axis. The tongue anlage has one pair of conical, often pustulate lingual papillae; some pustules may appear accompanying lingual papillae. The buccal floor arena is rounded or slightly hexagonal, delimited by 25–40 pairs of papillae symmetrically arranged in two lines that diverge anteroposteriorly, run caudally almost parallel to each other, and then converge on the medial region of the ventral velum anterior edge; the anterior papillae are small and simple, whereas the medial and posterior ones are larger and more developed, several also branched; papillae placed at the level of the buccal pockets are often joined at their base, resulting in wide, flat and deeply bifurcate papillae. Groups of tall, pustulate papillae diverge laterally, and locate on the

ceratohyal lateral region and following the anterior margin of the buccal pockets. A third arrangement includes papillae that are disposed following two lines that diverge lateral and anteriorly from the arena posterior edge, lining the ventral velum anterior margin. Numerous pustules and low papillae scatter among the main papillae and on the central region of the arena, posterior to the level of the buccal pockets. The buccal pockets are long and oriented transversal or slightly oblique regarding the body longitudinal axis. The ventral velum is long and thick, supported by spicules; it has 6 conspicuous marginal projections disposed on the filter plates, medially oriented; the most lateral projections are smaller and rounded, and the remaining are larger and pointed; on the medial region, there is a couple of projections on both sides of the small median notch, laterally oriented; in some specimens, there is a second pair of small projections placed between the median and the first marginal projections. Secretory pits appear on the posterior, ventral margin of the velum.

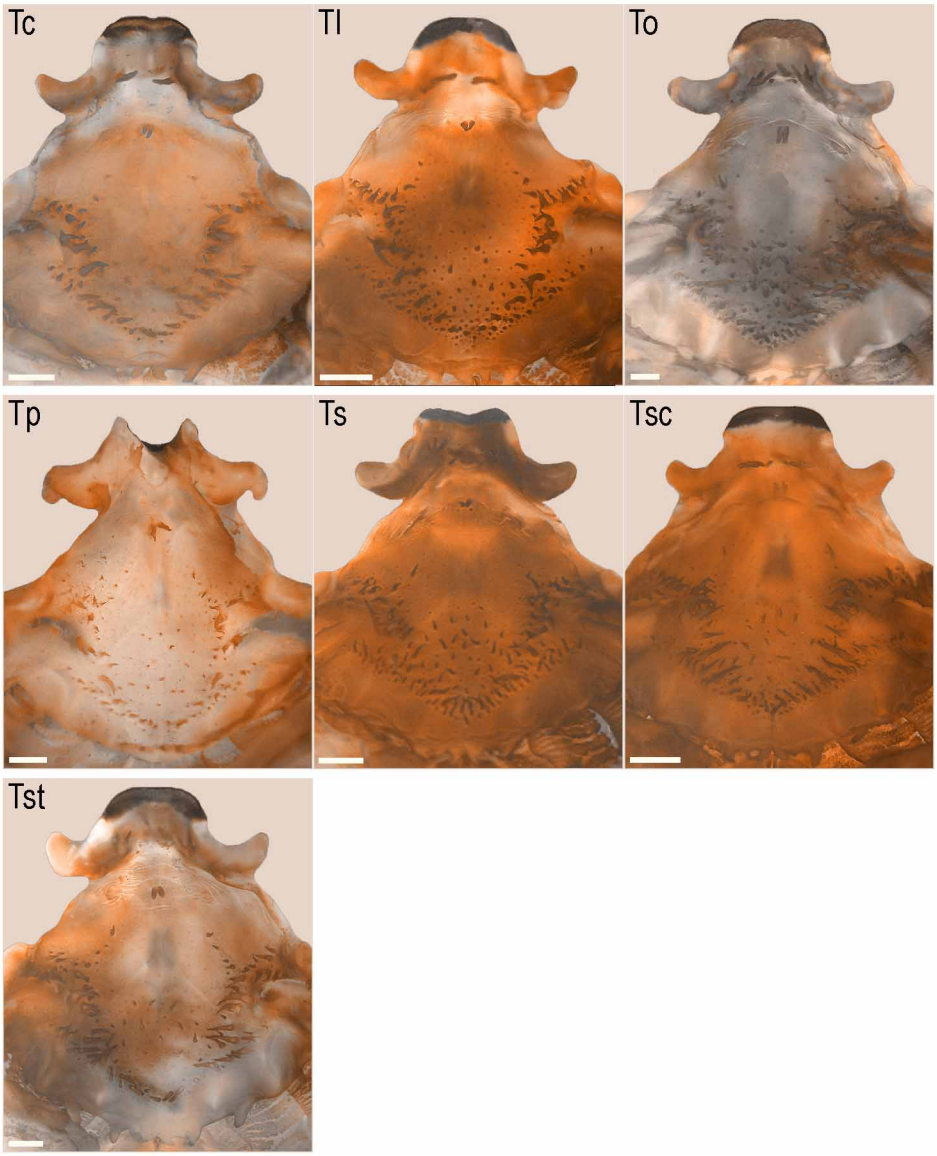

FIGURE 5. Buccal floors in other *Telmatobius*. Tc *T. ceiorum*, Tl *T. laticeps*, To *T. oxycephalus*, Tp *T. pinguiculus*, Ts *T.* cf. *schreiteri*, Tsc *T. scrocchii*, Tst *T. stephani*. *T. pisanoi* picture is not shown because after examination the specimen was too destroyed to be photographed. Scale lines = 1 mm.

Chondrocranium and hyobranchial skeleton. The chondrocranium of these larvae (Figs. 6 and 7) represents about 42% of the body length, and maximum width is at the level of the posterior region of the suboocular bar. The suprarostral cartilage is tetrapartite, formed of distinguishable corpora and alae. The corpus

portions are subtriangular, and are joined to each other by a connective commissure. The alae are quadrangular and show dorsal anterior and posterior processes well-developed. Next to the dorsal edge of each ala, there is a small and polyhedric adrostral cartilage; in some specimens of *Telmatobius atacamensis*, *T. laticeps*, *T. pisanoi*, and *T. stephani*, two chondrification centers are visible. The trabecular horns are long (22–26% of the chondrocranium total length), and have an oblique anterior edge. The lateral trabecular process is well-defined in some specimens of *T. pisanoi*, *T.* cf. *schreiteri*, and *T. stephani*. The nasal septum and the antorbital processes are developed, and the latter approach to the muscular process tip. The chondrocranium is dorsally open through the frontoparietal fenestra, lined on both sides by the taeniae tecti marginales. The chondrocranial lateral walls are represented by the orbital cartilages; oculomotor and optic foramina are visible, the latter

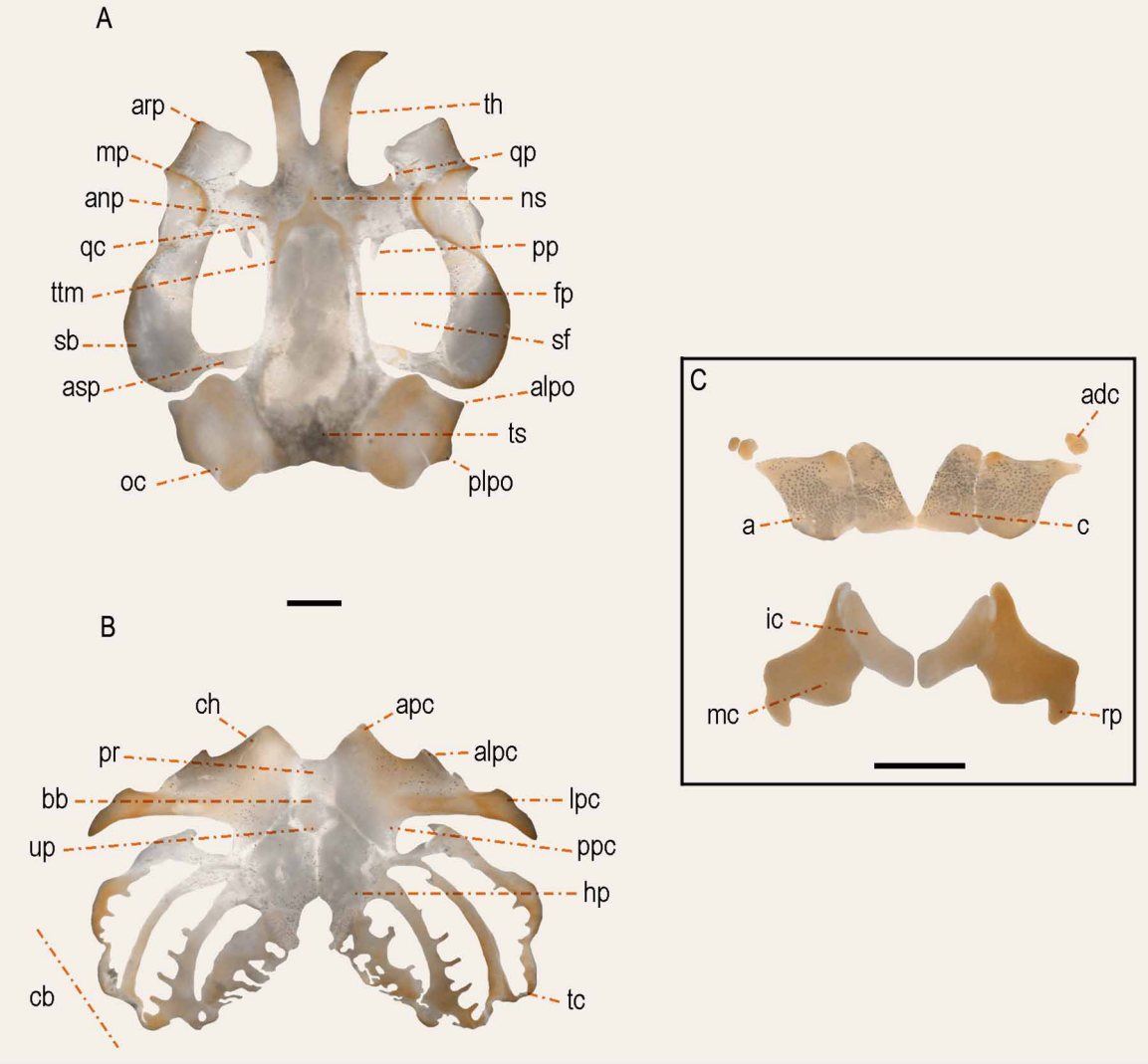

FIGURE 6. *Telmatobius atacamensis* chondrocranium and hyobranchial skeleton, stage 34. (A) Neurocranium, dorsal view (B) Hyobranchial skeleton, ventral view (C) Detail of upper and lower jaw cartilages, frontal and ventral views respectively. a ala, adc adrostral cartilage, alpc anterolateral process of ceratohyal, alpo anterolateral process of the otic capsule, anp antorbital process, apc anterior process of ceratohyal, arp articular process, asp ascending process, bb basibranchial, c corpus, cb(I-IV) ceratobranchial, ch ceratohyal, fp frontoparietal, hp hypobranchial plate, ic infrarostral cartilage, lpc lateral process of ceratohyal, mc meckel's cartilage, mp muscular process, ns nasal septum, oc otic capsule, plpo posterolateral process of the otic capsule, pp pseudopterygoid process, ppc posterior process of ceratohyal, pr pars reuniens, qc quadratocranial commissure, qp quadratoethmoid process, rp retroarticular process, sb subocular bar, sf subocular fenestra, tc terminal commissure, th trabecular horn, ts tectum synoticum, ttm taenia tecti marginalis, up urobranchial process. Scale lines = 1 mm.

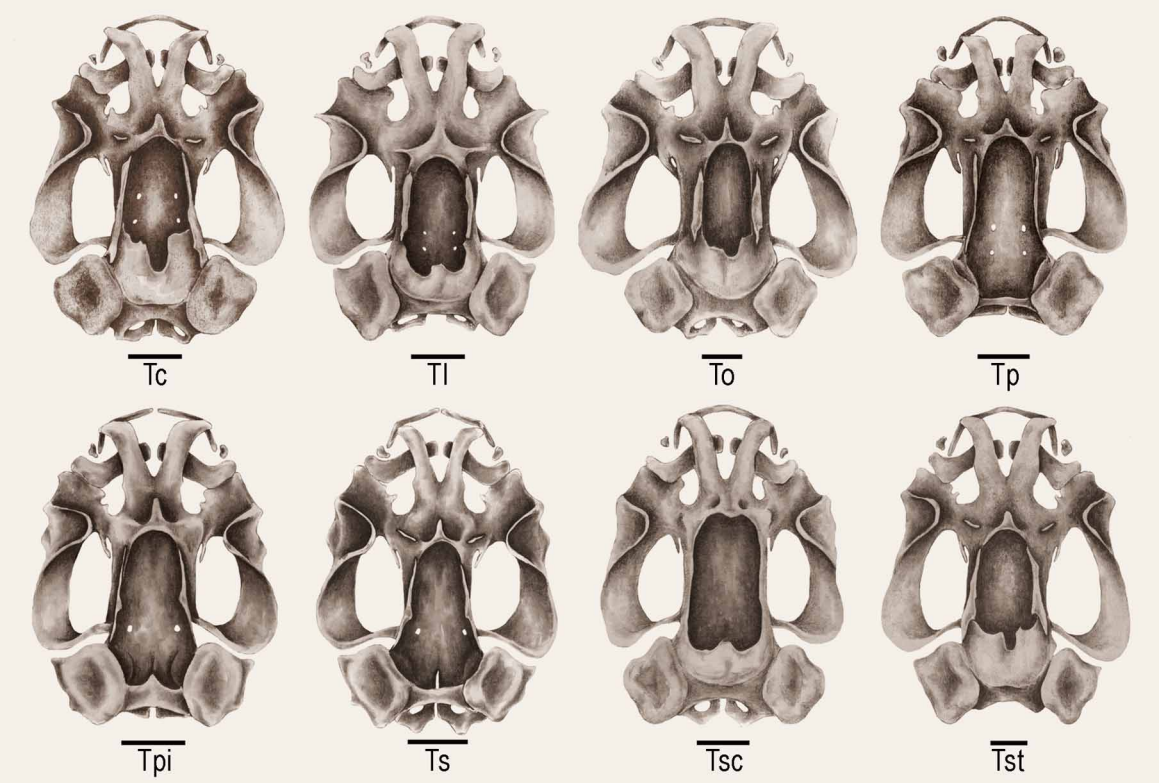

FIGURE 7. Chondrocrania in other *Telmatobius*. Tc *T. ceiorum*, Tl *T. laticeps*, To *T. oxycephalus*, Tp *T. pinguiculus*, Tpi *T. pisanoi*, Ts *T.* cf. *schreiteri*, Tsc *T. scrocchii*, Tst *T. stephani*. Scale lines = 1 mm.

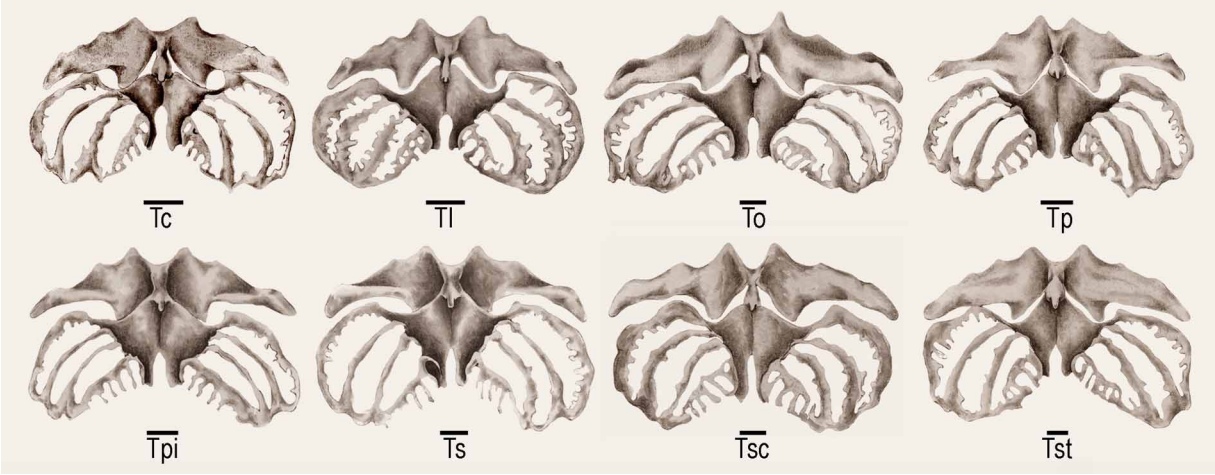

FIGURE 8. Hyobranchial skeletons in other *Telmatobius*. Tc *T. ceiorum*, Tl *T. laticeps*, To *T. oxycephalus*, Tp *T. pinguiculus*, Tpi *T. pisanoi*, Ts *T.* cf. *schreiteri*, Tsc *T. scrocchii*, Tst *T. stephani*. Scale lines = 1 mm.

slightly larger. The trochlear foramen is placed near the dorsal margin of the orbital cartilage, partially concealed by the frontoparietals. The prootic foramen appears between the orbital cartilage and the otic capsule. The cranial floor is completely cartilaginous; carotid and craniopalatine foramina are visible, the latter larger and medially placed. The otic capsules are quadrangular and occupy about 23–27% of the chondrocranial length; anterolateral processes are evident in *T. laticeps* and *T. stephani*, and both antero- and posterolateral processes appear in *T. atacamensis*, *T. pisanoi*, and *T.* cf. *schreiteri*. Otic capsules are joined to each other by the tectum synoticum; in some specimens of *T. atacamensis*, *T. ceiorum*, *T. laticeps*, *T. oxycephalus*, *T. scrocchii*, and *T. stephani*, a thin cranial roof develops. The fenestra ovalis represents about 37–42% of the capsule

length. The palatoquadrate cartilage is oriented slightly convergent to the body longitudinal axis. It has a wide and long articular process, a rounded muscular process medially inclined, and a smooth subocular bar slightly wider in its posterior region. From the anterior edge of the muscular process, a small, pointed process projects laterally, this process is well-developed in some specimens of *T. laticeps*, *T. oxycephalus*, *T. pisanoi*, and *T.* cf. *schreiteri*. Anteriorly, the palatoquadrate articulates with the neurocranium through the quadratocranial commissure, which has a triangular quadratoethmoid process (well-developed in some specimens of *T. ceiorum*, *T.* cf. *schreiteri*, and *T. pisanoi*) and a long, thin pseudopterygoid process, attached to the cranial floor (*T. oxycephalus*) or free (remaining species). The ascending process attaches to the neurocranium below the oculomotor foramen. In the lower jaw, Meckel's cartilages are long and sigmoid, and have a long, medially oriented retroarticular process, point of articulation with the palatoquadrate, and ventro- and dorsomedial processes articulating with the infrarostral cartilages. On the posterior margin, there is a rounded process lying on a small sinus in the palatoquadrate articular process; this process is well-developed in *T. atacamensis*, *T. laticeps*, *T.* cf. *schreiteri*, and *T. stephani*. The infrarostral cartilages are oblong, dorsally curved, and have a

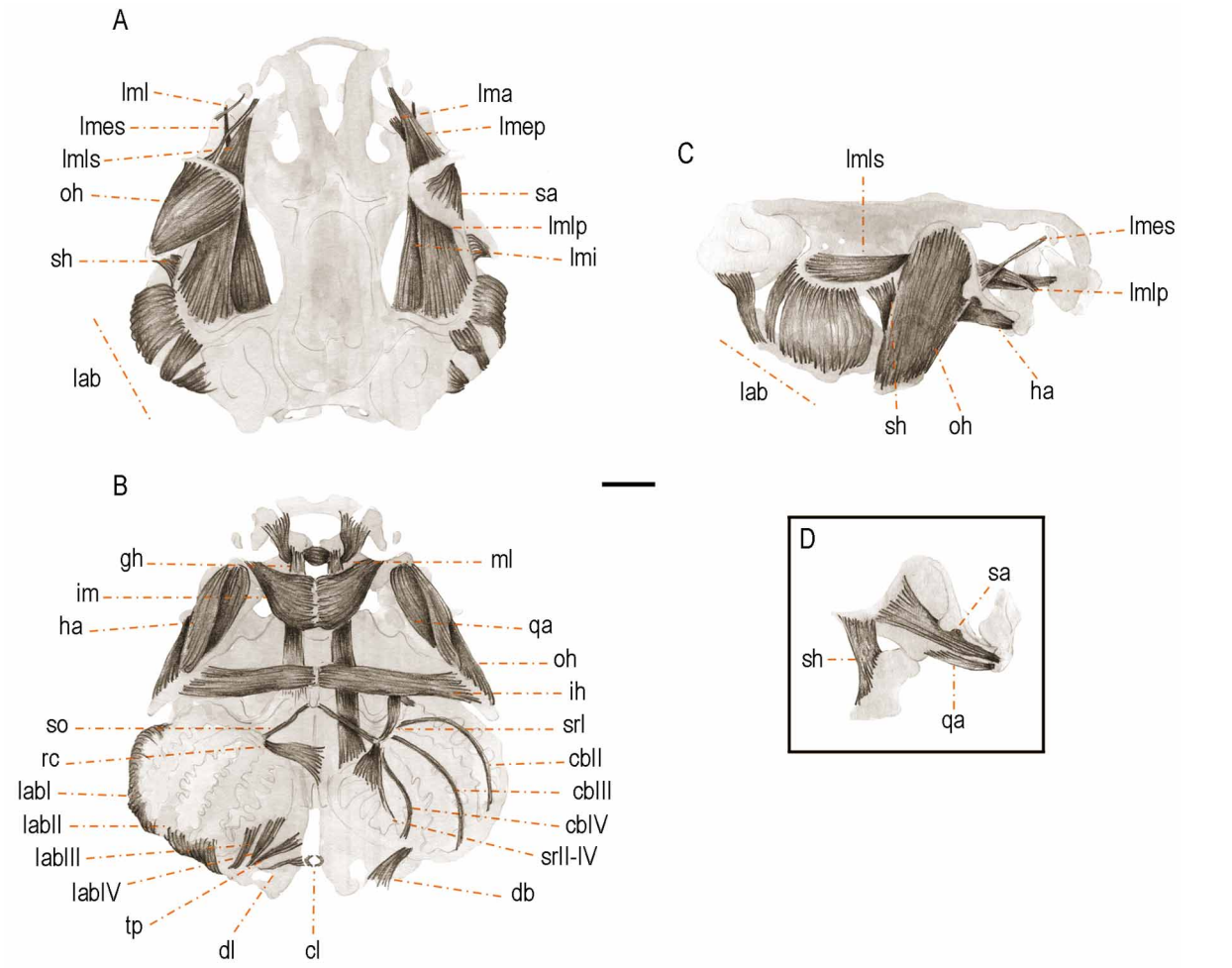

FIGURE 9. *Telmatobius laticeps* musculature, stage 31 (A) Dorsal view (B) Ventral view (C) Lateral view (D) Detail of the muscles of the muscular process; mm. orbitohyoideus and hyoangularis have been removed, in order to show the insertions of mm. quadratoangularis, suspensorioangularis, and suspensoriohyoideus. cb (II–IV) constrictor branchialis, cl constrictor laryngis, db diaphragmatobranchialis, dl dilatator laryngis, gh geniohyoideus, ha hyoangularis, ih interhyoideus, im intermandibularis, lab (I–IV) levator arcuum branchialis, lma levator mandibulae articularis, lmep levator mandibulae externus profundus, lmes levator mandibulae externus superficialis, lmi levator mandibulae internus, lml levator mandibulae lateralis, lmlp levator mandibulae longus profundus, lmls levator mandibulae longus superficialis, ml mandibulolabialis, oh orbitohyoideus, qa quadratoangularis, rc rectus cervicis, sa suspensorioangularis, sh suspensoriohyoideus, so subarcualis obliquus, sr (I–IV) subarcualis rectus, tp tympanopharyngeus. Scale line = 1 mm.

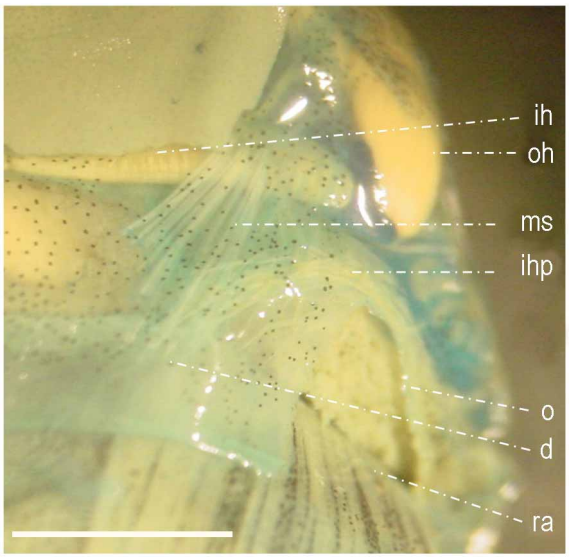

FIGURE 10. Detail of the diaphragm muscles, with the apparently typical disposition in *Telmatobius*. The photograph corresponds to *T. ceiorum*. d diaphragm, ms medial slip, ih interhyoideus, ihp interhyoideus posterior, o operculum, oh orbitohyoideus, ra rectus abdominis. Scale line = 1 mm.

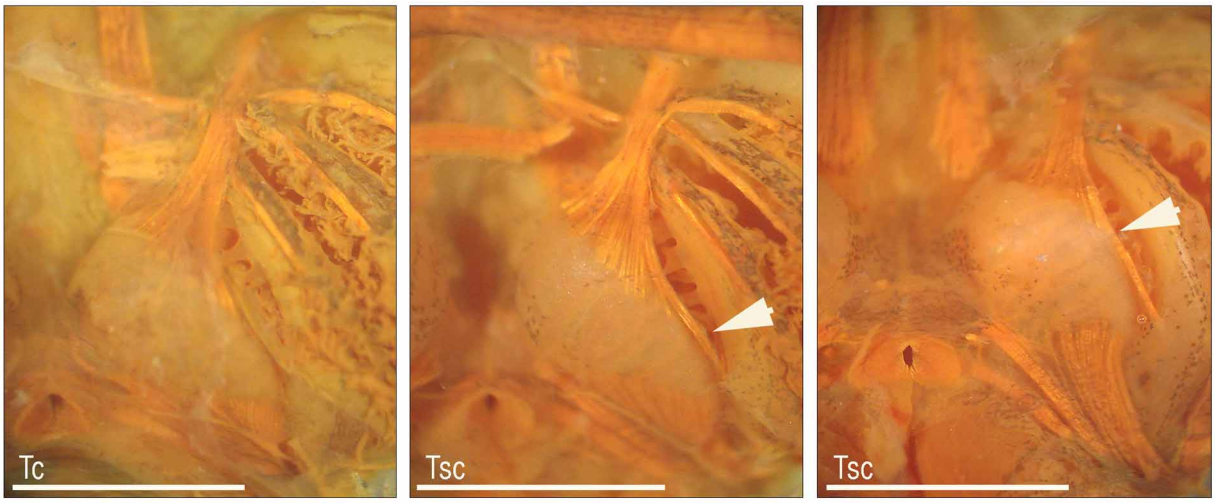

FIGURE 11. Detail of the m. subarcualis rectus II-IV, varied patterns in *Telmatobius*. Tc *T. ceiorum*, Tsc *T. scrocchii*. The arrows show the diverging muscle slips in *T. scrocchii*, discontinuous in the second specimen. Scale lines = 1 mm.

small notch on the posterior margin; they are joined to each other through a connective intramandibular commissure. Finally, regarding ossifications of the neurocranium, at the analyzed stages the frontoparietals appear as long, narrow structures placed dorsally to the taeniae tecti marginales. In the hyobranchial skeleton (Figs. 6 and 8), the ceratohyals are long and have conspicuous processes. On the anterior margin, there is a triangular, wide anterior process, a lower and medially oriented anterolateral process, and a small process placed near the edge of the ceratohyal. The anterior process is rounded in *T. laticeps* and *T.* cf. *schreiteri*, and pointed in the remaining taxa; the anterolateral process is short and smooth in *T. ceiorum*, tall and thin in *T. atacamensis*, and has an average development in the remaining species. On the posterior margin, a tall, triangular, laterally oriented posterior process is visible. Finally, a rounded articular condyle, point of articulation with the palatoquadrate, appears on the ceratohyal dorsal surface. The ceratohyals articulate medially through a quadrangular pars reuniens. The basihyal is absent, and the basibranchial is short and wide, and on its edge shows a wide, rounded urobranchial process (quadrangular in most specimens of *T. ceiorum*, *T.* cf. *schreiteri*, and *T. pisanoi*). The hypobranchial plates are flat, long, and articulate on the middle line, leaving an ovoid notch on the most

caudal portion; they are anteriorly fused to the basibranchial. The ceratobranchials are thin and curve, with numerous lateral projections on their margins. They are proximally joined to the hypobranchial plates through cartilaginous commissures, excepting the ceratobranchial I, which is fused to the hypobranchial. Distally, they are joined by terminal commissures. The ceratobranchial I has a wide, rounded anterior branchial process. In the ceratobranchial II, lateral projections are frequently less-developed than in the others. The ceratobranchial IV is wider and shorter. In the proximal edge of the ceratobranchials II and III, there is an open branchial process, where ceratobranchial projections face to each other without constituting a cartilaginous bridge. Three long, thin, curve spicules appear dorsally, and the fourth one is flat, wide and rectangular.

FIGURE 12. Detail of the mm. levator arcuum branchialium IV, tympanopharyngeus, and dilatator laryngis in *Telmatobius*. The photograph corresponds to *T. pinguiculus.* Scale line = 1 mm.

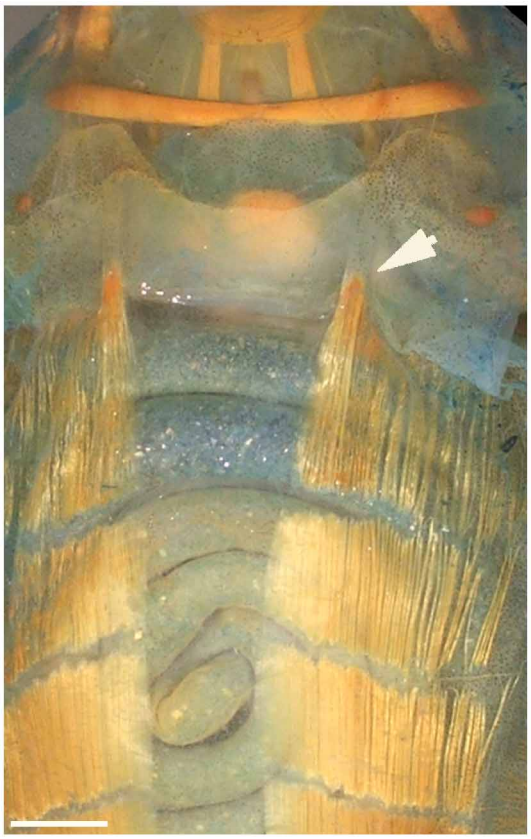

FIGURE 13. Detail of the m. rectus abdominis frequent pattern in *Telmatobius*, with a medial slip inserting on the ventral surface of the diaphragm and extending anteriorly reaching the palatoquadrate articular process (arrow**)**. The photograph corresponds to *T. pinguiculus*. Scale line = 1 mm.

TABLE 2. Larval musculature of *Telmatobius atacamensis.*

Muscle	Insertions	Comments and variations
Mandibular muscles		
Intermandibularis	medial region of the Meckel's cartilage – median aponeurosis	the whole structure has a U-shaped configuration
Levator mandibulae articularis	medial, inferior surface of the muscular process – dorsal region of the Meckel's cartilage	short and poorly developed
Levator mandibulae externus profundus	medial, inferior surface of the muscular process – lateroventral margin of the suprarostral ala	the anterior insertion is through a tendon common with that of the m. l. m. l. profundus
Levator mandibulae externus superficialis	medial, inferior surface of the muscular process – dorsal posterior process of the suprarostral ala	poorly developed, formed of 5–6 fibers; the branch V_3 of the trigeminal nerve runs dorsally to this muscle; the anterior insertion can be on mandibulosuprarostral ligament (*T. ceiorum*), connective tissue next to the adrostral cartilage (*T. laticeps*, *T.* cf. *schreiteri*, *T. scrocchii*), or posterior surface of the adrostral cartilage (*T. oxycephalus*, *T. pinguiculus*, *T. pisanoi*, *T. stephani*)
Levator mandibulae internus	ventral surface of the ascending process – distal edge of the Meckel's cartilage	the insertion on Meckel's cartilage is through a long tendon
Levator mandibulae lateralis	dorsal edge of the articular process –posterior surface of the adrostral cartilage	very thin, formed of few fibers; the anterior insertion can be on connective tissue next to the adrostral cartilage (*T. oxycephalus*, *T. stephani*).
Levator mandibulae longus profundus	external and posterior margin of the suboccular bar – external margin of the suprarostral ala	the surface of origin coincides with that of the m. l. m. l. superficialis
Levator mandibulae longus superficialis	external and posterior margin of the suboccular bar – mediodorsal region of the Meckel's cartilage	
Mandibulolabialis	ventromedial region of the Meckel's cartilage – lower labium of the oral disc	formed of a single slip, corresponding to the m. mandibulolabialis inferior
Submentalis	absent	present in studied specimens of *T. ceiorum*, *T. laticeps*, *T. oxycephalus*, and *T. stephani*, between infrarostral cartilages
Hyoid muscles		
Hyoangularis	dorsal surface of the ceratohyal – retroarticular process	
Interhyoideus	ventral surface of the ceratohyal – median aponeurosis	
Interhyoideus posterior + Diaphragmatopraecordialis	I couldn't dissect these two muscles in 8 of the 9 species studied. However, in *T. ceiorum* there appear two muscles in a characteristic pattern (Fig. 10): the lateral slip corresponds to the m. interhyoideus posterior, in its typical disposition lining the peribranchial chamber; the medial slip originates ventrally on the diaphragm, next to the m. interhyoideus posterior, and runs anteriorly to insert on connective tissue of the region surrounding the articular process. Histological studies would be required to verify if this pattern maintains in other species of the genus.	

.....continue

TABLE 2. (continued)

Muscle	Insertions	Comments and variations
Orbitohyoideus	anterior and dorsal margin of the muscular process – edge of the ceratohyal	
Quadratoangularis	ventral surface of the palatoquadrate – retroarticular process	in lateral view, it is concealed by the m. hyoangularis
Suspensorioangularis	inferior region of the descending margin of the muscular process – retroarticular process	the origin is concealed by the m. orbitohyoideus; fibers occupy the lower half of the muscular process
Suspensoriohyoideus	posterior descending margin of the muscular process – dorsal surface of the edge of the ceratohyal	
Branchial muscles		
Constrictor branchialis II	branchial process II – terminal commissure I	
Constrictor branchialis III	branchial process II – terminal commissure II	
Constrictor branchialis IV	branchial process II – terminal commissure III	in *T. pinguiculus*, the anterior insertion is on the branchial process III
Constrictor laryngis	sphincter-like disposition, surrounding the glottis	
Diaphragmatobranchialis	peritoneum – distal edge of the ceratobranchial III	
Dilatator laryngis	posterolateral, ventral region of the otic capsule – arytenoid cartilage	
Levator arcuum branchialium I	lateral margin of the subocular bar –lateral margin of the ceratobranchial I	
Levator arcuum branchialium II	lateral margin of the subocular bar and part of the ascending process – terminal commissure I	in *T. ceiorum*, the dorsal insertion reaches part of the otic capsule
Levator arcuum branchialium III	lateral region of the otic capsule – terminal commissure II	
Levator arcuum branchialium IV	posterolateral, ventral region of the otic capsule – medial region of the ceratobranchial IV	it shows a division into two slips
Subarcualis obliquus	urobranchial – branchial process II	
Subarcualis rectus I	two slips: region lateral to the base of the posterior hyal process – proximal region of the ceratobranchial I (dorsal slip) and branchial process II (ventral slip)	
Subarcualis rectus II-IV	branchial process II – proximal, ventral region of the ceratobranchial IV	a single slip (*T. pinguiculus*, *T. pisanoi*, *T. scrocchii*), or with some fibers slightly diverging towards the distal part of the ceratobranchial IV, invading the branchial septum IV (*T. ceiorum*, *T. laticeps*, *T. oxycephalus*, *T. pisanoi*, *T.* cf. *schreiteri*,

.....continue

TABLE 2. (continued)

Muscle	Insertions	Comments and variations
Subarcualis rectus II-IV	branchial process II – proximal, ventral region of the ceratobranchial IV	*T. scrocchii*, *T. stephani*). In one specimen of *T. pisanoi*, the muscle interrupts on the branchial process II, resulting in anterior and posterior portions. In one specimen of *T. scrocchii*, the diverging slip is discontinuous. Finally, in some specimens, some lateral fibers of the m. s. r. II-IV are continuous with those of the m. constrictor branchialis II (*T. pisanoi*, *T. scrocchii*, *T. stephani*), or those of the mm. c. b. II and III (*T.* cf. *schreiteri*) (Fig. 11).
Tympanopharyngeus	posterolateral, ventral region of the otic capsule – connective tissue of the pericardium	fibers diverge medially from the medial slip of the m. l. a. b. IV (Fig. 12)
Spinal muscles		
Geniohyoideus	posterior, ventral surface of the infrarostral – hypobranchial plate, next to the junction with the ceratobranchial IV	
Rectus abdominis	dorsal surface of the diaphragm – pelvic girdle	it shows a medial slip inserting on the ventral surface of the diaphragm, next to the insertion of the m. rectus cervicis, and extending far anteriorly to the palatoquadrate articular process (same condition in *T. oxycephalus*, *T. pinguiculus*, *T. pisanoi*, *T.* cf. *schreiteri*, *T. scrocchii*, and *T. stephani*) (Fig. 13)
Rectus cervicis	dorsal surface of the diaphragm –branchial process II	

The results of geometric morphometric analyses carried out show a marked overlapping among species and a high intraspecific variation. The ordination of species according to their chondrocranium plus hyobranchial skeleton shape is almost identical to that of the hyobranchial skeleton itself, suggesting that chondrocranium shape does not contribute significantly to shape variation. Figure 14 shows the scatterplot of species according to both structure shape, on the first three principal components (explained variance ≅ 41.5%); it can be noted that species are better discriminated along PC2, with *Telmatobius ceiorum*, *T. pisanoi*, *T. scrocchii*, and *T. oxycephalus* scoring high on the axis, *T. laticeps* and *T. pinguiculus* scoring low, and *T.* cf. *schreiteri*, *T. atacamensis* and *T. stephani* scattered among them. Shape change implies a slight enlargement of the branchial basket relative size, and a widening of the buccal pocket (this defined between the ceratohyal lateral process and the ceratobranchial I). On PC3, *T. stephani* diverges from *T. atacamensis* and *T.* cf. *schreiteri*. Regarding suprarostral cartilages (Fig. 15), *T. laticeps*, *T. ceiorum*, and *T. stephani* appear grouped in the morphospace defined by the three first ES axes (explained variance ≅ 50%), and their resemblance with *T.* cf. *schreiteri* on ES1-ES2 fades on ES3; ES3 also helps to discriminate among *T.* cf. *schreiteri*, *T. oxycephalus*, and *T. atacamensis*, and *T. pisanoi* from *T. scrocchii*. The apparent divergence of *T. pinguiculus* in both geometric morphometric analyses could be an artifact of having included only a single specimen. Figure 16 shows suprarostrals modeled on the first three eigenshapes, in order to interpret shape change; ES1 shows a change at the corpus-ala ventral junction, ES2 is mainly associated with alae shortening and dorsolateral process orientation, and ES3 reveals a slight change on corpus-ala dorsal junction.

Musculature. The musculature in these species includes 35 muscles: 10 mandibular (innerved by cranial pair V), 8 hyoid (pair VII), 14 branchial (pairs IX and X), and 3 spinal muscles (pair II) (Figs. 9–13). Table 2 summarizes main features of each muscle in *Telmatobius atacamensis*, and details some interspecifically variable characters.

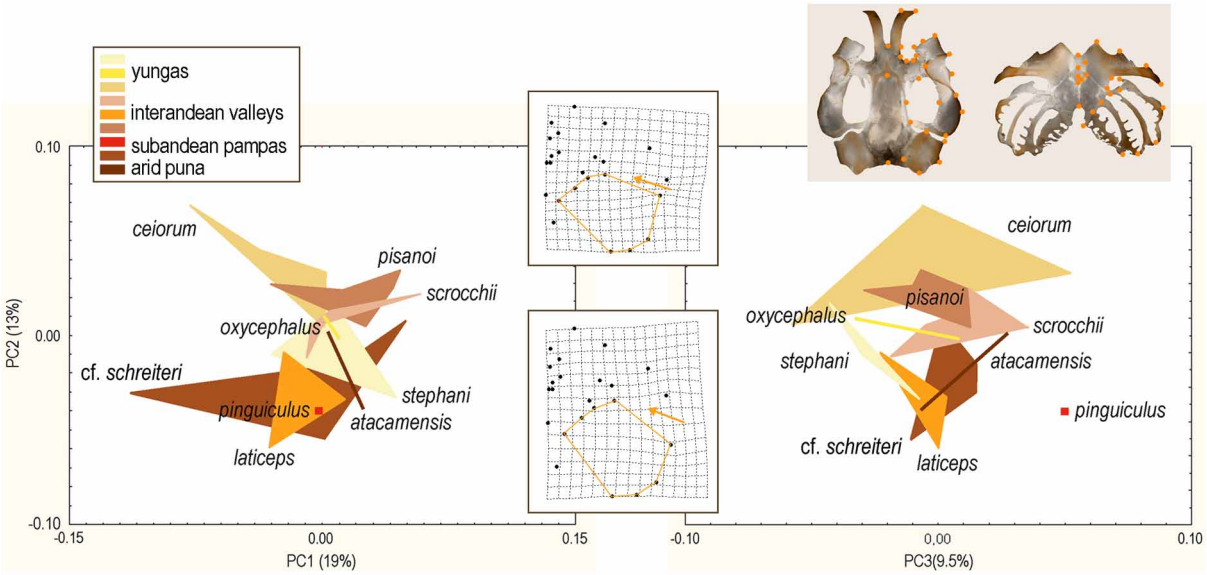

FIGURE 14. Principal component analysis on the combined matrices of chondrocranium and hyobranchial skeleton shape variables (almost identical to the PCA on the hyobranchial skeleton matrix). The discrimination of species is clearer on the PC2; grids depict modeled specimens on this axis, with maximum (top) and minimum (bottom) scores. Shape change implies a slight enlargement of the relative size of the branchial basket (enclosed area), and a widening of the buccal pocket (arrow). The classification according to biogeographical regions is based on Laurent (1970) and Olson *et al.* (1998).

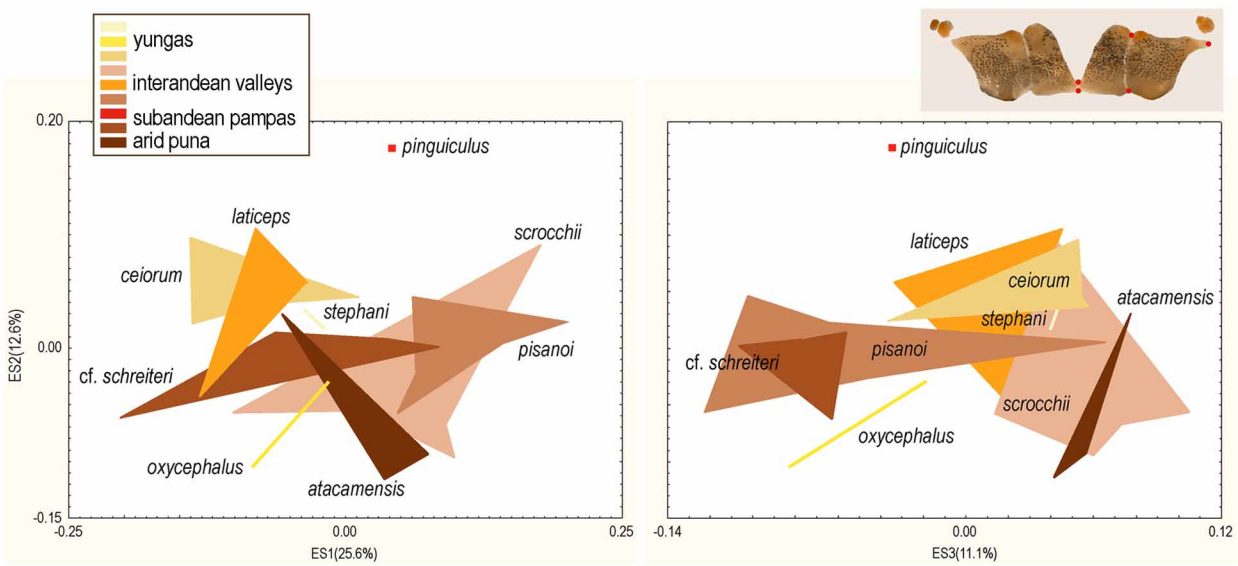

FIGURE 15. Extended eigenshape analysis on suprarostral cartilages. A high superposition among specimens is evident, and ES3 helps to discriminate species that overlap on ES1-ES2 morphospace. The classification according to biogeographical regions is based on Laurent (1970) and Olson *et al.* (1998).

Discussion

Oral morphology in the genus *Telmatobius* has been widely commented by previous researchers on species across the whole distribution (Trueb 1979; Díaz & Valencia 1985; Lavilla 1983; 1984; 1985; 1988; Lavilla & De la Riva 1993; Cuevas & Formas 2002; De la Riva & Harvey 2003; Formas *et al*. 2003; compilations by De

la Riva 2005, Formas *et al.* 2005; Lavilla & Barrionuevo 2005, Lehr 2005, and Merino-Viteri *et al.* 2005, and references in those chapters; Aguilar 2006; Formas *et al.* 2006; Aguilar *et al.* 2007). All described forms share a not emarginated (transangular, sensu Lavilla 1988) oral disc, surrounded by a complete (*T. atahualpai*) or dorsally interrupted (remaining species) papillar margin. Commissural submarginal papillae appear in different patterns in these species, including papillae present only in the supraangular region (e.g., *T. espadai*), only in the infraangular region (*T. atahualpai*), or constituting a continuous band mainly concentrated in the angular region, frequently extending to supra - and infraangular regions (remaining species from Bolivia and Perú, and Argentinean, Chilean and Ecuadorian species described). Lavilla (1985) proposed a division of the genus into meridional and septentrional groups, subject to lower submarginal papillae being present (Argentinean species, *T. atahualpai*, *T. brevirostris*, *T. espadai*, *T. yuracare*, *T. vilamensis*, *T. rimac*) or absent (remaining described tadpoles from Bolivia, Chile, Perú, and Ecuador). Regarding the morphology of keratinized structures, most species have curved, well-keratinized, serrated rostrodonts, and labial teeth arranged according to a 2(2)/3(1) labial tooth row formula. *Telmatobius atahualpai* tadpoles constitute the only exception so far, with unusual formulae 3/6(1) and 3/7(1). Labial tooth configuration had not been explored in the genus before; species here studied show a typical labial tooth morphology: head with 10–14 cusps, short body, and a wide sheath. Finally, the occurrence of labial teeth on papillae has been mentioned in other species (e.g., Altig & McDiarmid 1999a; Alcalde *et al.* 2006; Borteiro & Kolenc 2007), and represents further evidence supporting the idea about papilla and labial ridge homology (Altig 2006).

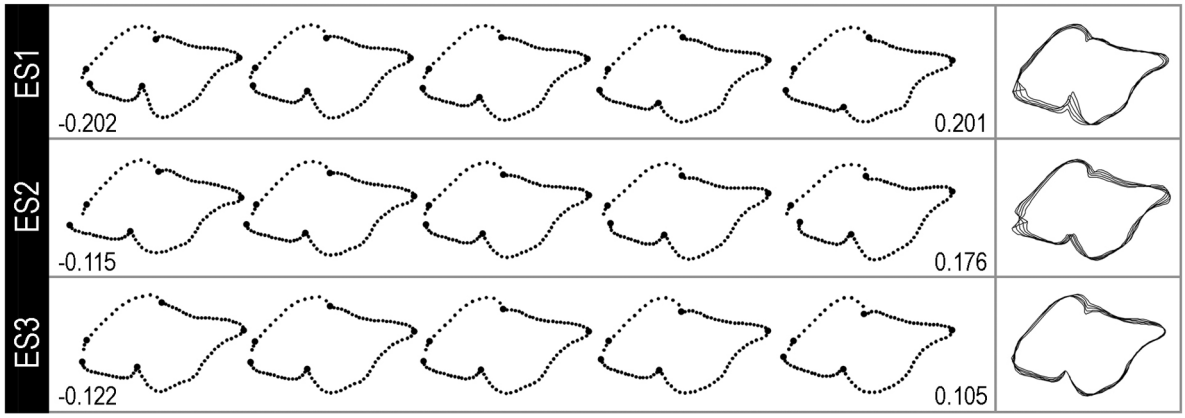

FIGURE 16. Modeled suprarostrals along the first three eigenshapes, at minimum, 25%, 50%, 75%, and maximum scores. Open curves, more evident on ES2 models, are due to the modeling technique, which generates mathematically constructed shapes (MacLeod 1999; Krieger *et al.* 2007). Figures within the squares at right show overlapped curves to highlight places where the shape change is more evident: ES1 shows a change at the corpus-ala ventral junction, ES2 is mainly associated with alae shortening and dorsolateral process orientation, and ES3 reveals a slight change on corpus-ala dorsal junction. Note also the minimum number of points calculated by EEA to describe each outline segment (i.e., 3, 13, 23, 28, and 19).

The buccopharyngeal morphology of the studied species is very conservative, with a distinct combination of characters. On the buccal roof, species share the barely naked prenarial arena, 3–5 pairs of postnarial papillae in an inverted-V pattern, one pair of pustules or low papillae anterior to the median ridge, well-developed, multifid lateral ridge papillae, a characteristic arrangement of buccal roof papillae –with a first group lining the arena lateral and posteriorly, and a second group laterally divergent–, a conspicuous glandular zone, and a short, medially interrupted dorsal velum. The buccal floors have one pair of small, bicuspidate spurs, two pairs of unevenly-developed infralabial papillae, two lingual papillae, a characteristic arrangement of the buccal floor papillae –with a first group lining the arena, a second group following the buccal pocket anterior margin, and a third group following the ventral velum anterior margin–, and a well-developed velum with spicular support, median notch, marginal projections, and secretory pits. Peruvian species described, even the

highly specialized rheophilous tadpole of *Telmatobius atahualpai*, have almost identical features (Wassersug & Heyer 1988; Aguilar & Pacheco 2005; Aguilar 2006; Aguilar *et al.* 2007).

The skeletons are very similar as well, with common characters such as the tetrapartite suprarostral, adrostral cartilages, quadratoethmoid process, long pseudopterygoid process, free or attached to the neurocranium floor, absent larval otic process, crista parotica often with antero- and posterolateral processes, and mostly generalized hyobranchial skeleton. There are no significant differences regarding previous descriptions of *Telmatobius ceiorum*, *T. laticeps*, and *T. pisanoi* (Fabrezi & Lavilla 1993). Aguilar (2006) carried out a phylogenetic analysis of 15 Peruvian species (including two *Batrachophrynus* species proposed to be integrated to *Telmatobius*) using, among others, larval skeletal characters; this author found features similar to those of the species here considered, and suggested the non-straight anterior edge of the trabecular horns and the absence of quadratoorbital commissure to be genus synapomorphies. In geometric morphometric analyses carried out, results show a marked overlapping among species and a high intraspecific variation. The configuration of the chondrocranium does not appear to contribute significantly to shape variation; regarding hyobranchial skeleton (Fig. 14), *Telmatobius ceiorum*, *T. pisanoi*, *T. scrocchii*, and *T. oxycephalus* tend to show smaller branchial baskets and narrower buccal pockets than the remaining species. Suprarostral cartilages of *T. laticeps*, *T. ceiorum*, and *T. stephani* have well delimited alae with dorsolateral processes acuter than those of other taxa (Figs. 15 and 16). Some ordinations maintain on both geometric morphometric analyses, such as the grouping of *T. laticeps* and *T. stephani*, *T. pisanoi* and *T. scrocchii*, and the placement of *T. stephani* and *T. atacamensis*, intermediate between *T. scrocchii* and *T.* cf. *schreiteri*. It is interesting to note that *T. pisanoi* and *T. laticeps*, very similar in adult morphology (Lavilla & Barrionuevo 2005), are consistently separated in larval skeletal morphology. Finally, there is no clear pattern of morphological distinction completely coincident with biogeographic distribution of *Telmatobius* species according to Laurent (1970) and Olson *et al.* (1998), but some observations are noteworthy. Species of Laurent's High Andean complex (including arid Puna and Subandean pampas: *T. atacamensis*, *T.* cf. *schreiteri*, and *T. pinguiculus*) tend to group in chondrocranium plus hyobranchial skeleton ordination; among Interandean valley taxa, *T. pisanoi* and *T. scrocchii* are more similar to each other than to *T. laticeps*, and can be told apart according to suprarostral morphology; lastly, there appears to be a trend for Yungas species to group in skeletal morphospace. All these very preliminary results should be confirmed after the analysis of wider samples that take into account intraspecific variation (at ontogenetic, interpopulational levels, etc.).

Species studied have a similar muscular configuration. Common features are the single slip of the m. mandibulolabialis, mm. levatores mandibulae externus superficialis and profundus, m. l. m. lateralis, m. subarcualis rectus I with two slips, compact and thin m. tympanopharyngeus, m. rectus abdominis often with a medial slip inserted on the diaphragm ventral surface and extending far anteriorly, and a lateral slip of the m. subarcualis rectus II-IV frequently invading the branchial septum IV. The diaphragm muscle pattern seen in *Telmatobius ceiorum* still needs to be verified in the remaining species. A previous study on an Argentinean *Telmatobius* showed similar results (Palavecino 1999), and Carr and Altig (1991) reported the absence of m. mandibulolabialis in *T.* sp. Noble (1929) interpreted the muscle slip disposed between the palatoquadrate anterior region and the diaphragm of *Amolops ricketti* tadpoles (very similar to *T. ceiorum* configuration) to be a second slip of the m. interhyoideus posterior; since the author also identified the m. diaphragmatopraecordialis in these torrent tadpoles, this consideration seems probable. Developmental studies could clarify this homology issue; in this case, the m. diaphragmatopraecordialis would be absent in *Telmatobius*. An interesting observation is that when the medial slip of the m. rectus abdominis is lifted, this diaphragmatic muscle also lifts, showing that both muscles are connected, and that the effective insertion of m. rectus abdominis reaches far anteriorly, at the level of the articular process of the palatoquadrate. Noble (1929) mentioned a subbranchial (interhyoideus posterior) musculature continuous with the m. rectus abdominis in mountain-brook tadpoles of *Heleophryne rosei*, and a m. rectus abdominis inserting far anteriorly on the palatoquadrate or Meckel's cartilage are found in lotic tadpoles of *Ascaphus truei* (Gradwell 1973), *Boophis*, *Hyloscirtus*,

Litoria (Haas & Richards 1998), and burrowing tadpoles of *Otophryne robusta* (Wassersug & Pyburn 1987) and *Leptobrachella mjobergi* (Haas *et al*. 2006). Finally, the m. s. r. II-IV with the diverging lateral slip is similar to the typical arrangement in Bufonidae (e.g., Haas 2003; Vera Candioti 2007).

Telmatobius tadpoles develop in several types of Andean aquatic environments, e.g., in Argentina, Lavilla and Barrionuevo (2005) mentioned the rhithron portion of lotic environments, thermal waters, and high Andean phanerogam peat bogs, and in Bolivia, some species appear also in lacustrine systems. Despite that, larval morphology appears to be conservative enough to preclude attempts to relate microhabitat and morphology, at least at the analyzed levels. Exceptions would be the specialized rheophilous larvae of *T. espadai*, *T. atahualpai*, and apparently *T. sanborni* and *T. verrucosus* (Lavilla & De la Riva 1993; De la Riva 2005; Aguilar *et al*. 2007). These forms have wide oral discs modified into functional oral suckers, in *T. atahualpai*, also with supernumerary labial ridges and a complete papillar margin. At a skeletal level, even when several characters are shared with other *Telmatobius*, some subtle differences appear. In *T. espadai* and *T. atahualpai*, for instance, the suprarostrals are tripartite, with fused corpora, the articular process is short and wide, and the palatoquadrate runs parallel to the chondrocranium longitudinal axis (corresponding traits in other species are a tetrapartite suprarostral, longer and narrower articular process, and palatoquadrates slightly convergent towards the middle axis). These features are surely correlated with the relatively wider oral disc employed in substrate fixation. In the hyobranchial skeleton, differences, if any, are also subtle: in-lever arm ratio (taken as the projected width of the lateral part of the ceratohyal to its total width; Wassersug & Hoff 1979) is around 0.25 in all species, the ceratobranchial area is similar to the species here studied, although among the smaller values, along with those of *T. oxycephalus*, *T. pisanoi*, and *T. scrocchii* (47–48% of the total area vs. 50–53%), the ceratohyal area is among the larger values, along with that of *T. oxycephalus* (34–36% vs. 31–33%), and finally, the ceratohyal tends to orient more inclined than in other species (59–66º regarding the longitudinal axis vs. 68–72º). Some of these skeletal features can be found also in other lotic tadpoles (e.g., Haas & Richards 1998; Aguayo *et al*. in prep.). Lastly, the configuration of the m. rectus abdominis found in most *Telmatobius* analyzed, in other species often appears associated with specific locomotor habits (e.g., living in fast-flowing streams, burrowing).

As a final comment, the conservative larval internal morphology in *Telmatobius* genus could be explained by recent speciation events, correlated with the relatively recent age of the Andes (Maxson & Heyer 1982), and an ontogenetic development possibly characterized by a postmetamorphic appearance of specific features. In most species, numerous morphological characters (e.g., body shape, configuration of the oral disc and buccopharyngeal cavity, several skeletal and muscular traits) coincide with features usually mentioned in pond-type larvae (e.g., Wassersug & Heyer 1988; Altig & McDiarmid 1999b; Lavilla & Barrionuevo 2005), although some of them resemble traits found in lotic tadpoles (e.g., some characteristics in the hyobranchial skeleton, configuration of the m. rectus abdominis). The appearance of these latter features in these mostly lentic, generalized species could be maybe explained from a phylogenetic frame; in this regard, more data about larval morphology in other related ceratophryids (e.g., *Batrachyla*, *Atelognathus*), and comprehensive phylogenetic analyses on the genus (e.g., Barrionuevo in prep.) would be required.

Acknowledgements

This work was supported by a CONICET (Consejo Nacional de Investigaciones Científicas y Técnicas) Post-doctoral Fellowship, carried out at the Instituto de Herpetología – Fundación Miguel Lillo, and CONICET PIP Nº 5780 and UNT (Universidad Nacional de Tucumán) CIUNT-G315 funds. I thank E. Lavilla and S. Kretzschmar for the access to specimens at the FML Herpetological Collection. I would also like to thank N. MacLeod and J. Krieger for sharing specific software for extended eigenshape analysis, along with very kind answers, comments and relevant explanations. I am indebted with S. Barrionuevo, for sharing tadpoles, litera-

ture, comments, and his overall expertise on these frogs. Finally, I thank an anonymous reviewer for suggestions and corrections that improved this manuscript.

References

Aguayo, R., Lavilla, E.O. & Vera Candioti, M.F. (---) The gastromyzophorous tadpole of *Rhinella quechua* (Anura: Bufonidae). In preparation.

Aguilar, C.A. (2006) *Relaciones filogenéticas entre algunos telmatobínidos (Anura, Leptodactylidae, Telmatobiinae) de Perú, basado en la morfología de los estados larval y adulto.* Ph.D. Dissertation, Universidad Nacional Mayor de San Marcos, Perú.

Aguilar, C.A. & Pacheco, V. (2005) Contribución de la morfología bucofaríngea larval a la filogenia de *Batrachophrynus* y *Telmatobius*. *Monografías de Herpetología*, 7, 219–238.

Aguilar, C.A., Siu-Ting, K. & Venegas, P. (2007) The rheophilous tadpole of *Telmatobius atahualpai* Wiens, 1993 (Anura: Ceratophryidae). *South American Journal of Herpetology*, 2, 165–174.

Alcalde, L., Natale, G.S. & Cajade, R. (2006) The tadpole of *Physalaemus fernandezae* (Anura: Leptodactylidae). *Herpetological Journal*, 16, 203–211.

Altig, R. (2006) Discussions of the origin and evolution of the oral apparatus of anuran tadpoles. *Acta Herpetologica*, 2, 95–105.

Altig, R. (2007) A primer for the morphology of anuran tadpoles. *Herpetological Conservation and Biology*, 2, 71–74.

Altig, R. & McDiarmid, R.W. (1999a) Body Plan: Development and morphology. *In:* McDiarmid, R.W. & Altig, R. (Eds.), *Tadpoles. The biology of anuran larvae*. University of Chicago Press, Chicago and London, pp. 24–51

Altig, R. & McDiarmid, R.W. (1999b) Diversity. Familial and generic characterization. *In:* McDiarmid, R.W. & Altig, R. (Eds.), *Tadpoles. The biology of anuran larvae*. University of Chicago Press, Chicago and London, pp. 295–337.

Barrionuevo, J.S. (---) *Análisis filogenético de las especies del grupo meridional del género Telmatobius (Anura: Leptodactylidae)*. Doctoral Thesis manuscript in preparation. Universidad Nacional de Tucumán, Argentina.

Borteiro, C. & Kolenc, F. (2007) Redescription of the tadpoles of three species of frogs from Uruguay (Amphibia: Anura: Leiuperidae and Leptodactylidae), with notes on natural history. *Zootaxa*, 1638, 1–20.

Carr, K.M. & Altig, R. (1991) Oral disc muscles of anuran tadpoles. *Journal of Morphology*, 208, 271–277.

Cei, J.M. (1980) Amphibians of Argentina. *Monitore Zoologico Italiano, Monografía* 2, 1–609.

Cei, J.M. (1986) Speciation and adaptive radiation in andean *Telmatobius* frogs. *In:* Vuilleumier, F. & Monasterio, M. (Eds.), *High Altitude Tropical Biology*. Oxford University Press, pp. 374–386.

Córdova, J.H. & Descailleaux, J. (2005) El análisis cladístico preliminar de los cariotipos de cinco especies de *Telmatobius* y dos de *Batrachophrynus* no apoya su separación genérica. *Monografías de Herpetología*, 7, 187–217.

Cuevas, C.C. & Formas, J.R. (2002) *Telmatobius philippii*, una nueva especie de rana acuática de Ollage, norte de Chile (Leptodactylidae). *Revista Chilena de Historia Natural*, 75, 245–258.

De la Riva, I. (2005) Bolivian frogs of the genus *Telmatobius*: synopsis, taxonomic comments, and description of a new species. *Monografías de Herpetología*, 7, 65–101.

De la Riva, I. & Harvey, M.B. (2003) A new species of *Telmatobius* from Bolivia and a redescription of *T. simonsi* Parker, 1940 (Amphibia: Anura: Leptodactylidae). *Herpetologica*, 59, 127–142.

Díaz, N.F. & Valencia, J. (1985) Larval morphology and phenetic relationships of the Chilean *Alsodes*, *Telmatobius*, *Caudiverbera* and *Insuetophrynus* (Anura: Leptodactylidae). *Copeia*, 1985, 175–181.

Fabrezi, M. & Lavilla, E.O. (1993) Anatomía del condrocráneo en larvas de tres especies de *Telmatobius* del grupo meridional (Anura: Leptodactylidae). *Physis*, 48B, 39–46.

Formas, J.R., Benavides, E. & Cuevas, C. (2003) A new species of *Telmatobius* (Anura: Leptodactylidae) from Río Vilama, Northern Chile, and the redescription of *T. halli* Noble. *Herpetologica*, 59, 253–270.

Formas, J.R, Cuevas, C.C. & Nuñez, J.J. (2006) A new species of *Telmatobius* (Anura: Leptodactylidae) from Northern Chile. *Herpetologica*, 62, 173–183.

Formas, J.R., Veloso, A. & Ortiz, J.C. (2005) Sinopsis de los *Telmatobius* de Chile. *Monografías de Herpetología*, 7, 103–114.

Frost, D.R. (2008) *Amphibian Species of the World: an Online Reference. Version 5.1 (10 October, 2007)*, American Museum of Natural History, New York, USA. Available from: http://research.amnh.org/herpetology/amphibia/index.php (accessed May 2008).

Frost, D.R., Grant, T., Faivovich, J., Bain, R.H., Haas, A., Haddad, C.F.B., De S, R., Channing, A., Wilkinson, M., Donnellan, S.C., Raxworthy, C.J., Campbell, J.A., Blotto, B.L., Moler, P., Drewes, R.C., Nussbaum, R.A., Lynch, J.D., Green, D.M. & Wheeler, W.C. (2006) The amphibian tree of life. *Bulletin of the American Museum of Natural History*, 297, 1–370.

Gosner, K.L. (1960) A simplified table for staging anuran embryos and larvae with notes on identification. *Herpetologica*, 16, 183–190.
Gradwell, N. (1973) On the functional morphology of suction and gill irrigation on the tadpole of *Ascaphus*, and notes on hibernation. *Herpetologica*, 29, 84–93.
Haas, A. (2003) Phylogeny of frogs as inferred from primarily larval characters (Amphibia: Anura). *Cladistics*, 19, 23–89.
Haas, A. & Richards, S.J. (1998) Correlations of cranial morphology, ecology and evolution in australian suctorial tadpoles of the genera *Litoria* and *Nyctimystes* (Amphibia: Anura: Hylidae: Pelodryadinae). *Journal of Morphology*, 238, 109–141.
Haas, A., Hertwig, S. & Das, I. (2006) Extreme tadpoles: the morphology of the fossorial megophryid larva, *Leptobrachella mjobergi*. *Zoology*, 109, 26–42.
Heyer, W.R. (1975) A preliminary analysis of the intergeneric relationships of the frog family Leptodactylidae. *Smithsonian Contributions to Zoology*, 199, 1–55.
Krieger, J.D., Guralnick, R.P. & Smith, D.M. (2007) Generating empirically determined, continuous measures of leaf shape for paleoclimate reconstruction. *Palaios*, 22, 212–219.
Kuhl, F.P. & Giardina, C.R. (1982) Elliptic Fourier features of a closed contour. *Computer Graphics Image Processing* 18, 236–258.
Laurent, R.F. (1970) Contribución a la biometría de algunas especies argentinas del género *Telmatobius*. *Acta Zoologica Lilloana*, 25, 279-302.
Laurent, R.F. (1973) Nuevos datos sobre el género *Telmatobius* en el noroeste argentino, con la descripción de una nueva especie de la Sierra del Manchao. *Acta Zoologica Lilloana*, 30, 163–187.
Laurent, R.F. (1977) Contribución al conocimiento del género *Telmatobius*. *Acta Zoologica Lilloana*, 32, 189–206.
Laurent, R.F. (1979) El origen de los anfibios sudamericanos. *Acta Zoologica Lilloana*, 24, 83–89.
Lavilla, E.O. (1983) *Sistemática de larvas de Telmatobiinae (Anura: Leptodactylidae)*. Ph.D. Dissertation, Universidad Nacional de Tucumán, Argentina.
Lavilla, E.O. (1984). Larvas de *Telmatobius* (Anura: Leptodactylidae) de la provincia de Tucumán (Argentina). *Acta Zoologica Lilloana*, 38, 69–79.
Lavilla, E.O. (1985). Diagnosis genérica y agrupación de las especies de *Telmatobius* (Anura: Leptodactylidae) en base a caracteres larvales. *Physis Sección B*, 43, 63–67.
Lavilla, E.O. (1988). Lower Telmatobiinae (Anura: Leptodactylidae): generic diagnoses based on larval characters. *Occasional Papers Museum Natural History, University of Kansas*, 124, 1–19.
Lavilla, E.O. (2005) Lista sistemática y bibliografía comentada sobre el género *Telmatobius*. *Monografías de Herpetología*, 7, 283–349.
Lavilla, E.O. & Barrionuevo, J.S. (2005) El género *Telmatobius* en la República Argentina: una síntesis. *Monografías de Herpetología*, 7, 115–165.
Lavilla, E.O. & De la Riva, I. (1993) La larva de *Telmatobius bolivianus* (Anura, Leptodactylidae). *Alytes*, 11, 37–46.
Lavilla, E.O. & Laurent, R.F. (1988a) Deux nouvelles espèces du genre *Telmatobius* (Anura: Leptodactylidae) en provenance de El Moreno (Province de Jujuy, Argentine). *Alytes*, 7, 77–89.
Lavilla, E.O. & Laurent, R.F. (1988b). A new species of *Telmatobius* (Anura: Leptodactylidae) from Catamarca, Argentina. *Alytes*, 7, 90–96.
Lavilla, E.O. & Scrocchi, G.J. (1986) Morfometría larval de los géneros de Telmatobiinae (Anura: Leptodactylidae) de Argentina y Chile. *Physis Sección B*, 44, 39–43.
Lehr, E. (2005) The *Telmatobius* and *Batrachophrynus* species of Perú. *Monografías de Herpetología*, 7, 39–64.
Lohmann, G.P. (1983) Eigenshape analysis of microfossils: a general morphometric procedure for describing changes in shape. *Mathematical Geology*, 15, 659–672.
Lynch, J.D. (1971) Evolutionary relationships, osteology and zoogeography of leptodactyloid frogs. *Miscellaneous Publications Museum Natural History, University of Kansas*, 53, 1–218.
Lynch, J.D. (1978) A re-assessment of the telmatobiine leptodactyloid frogs of Patagonia. *Occasional Papers Museum Natural History, University of Kansas*, 72, 1– 57.
MacLeod, N. (1999) Generalizing and extending the eigenshape method of shape space visualization and analysis. *Paleobiology*, 25, 107–138.
Maxson, L.R. & Heyer, W.R. (1982) Leptodactylid frogs and the Brasilian shield: an old and continuing adaptive relationship. *Biotropica*, 14, 10–15.
Merino-Viteri, A., Coloma, L.A. & Almendáriz, A. (2005) Los *Telmatobius* de los Andes de Ecuador y su disminución poblacional. *Monografías de Herpetología*, 7, 9–37.
Monteiro, L.R. & Furtado dos Reis, S. (1999) *Princípios de morfometria geométrica*, Brasil, Holos Editora Ltda-Me, 188pp.
Montero, R. & Pisanó, A. (1990) Ciclo espermatogénico de dos especies de *Telmatobius* del Noroeste Argentino. *Amphibia-Reptilia*, 11, 97–110.

Noble, G.K. (1929) The adaptive modifications of the arboreal tadpoles of *Hoplophryne* and the torrent tadpoles of *Staurois*. *Bulletin of the American Museum of Natural History*, 58, 291–337.

Olson, D., Dinerstein, E., Canevari, P., Davidson, I., Castro, G., Morisset, V., Abell, R. & Toledo, E. (1998) *Freshwater Biodiversity of Latin America and the Caribbean: A Conservation Assessment*. Biodiversity Support Program, Washington, D.C.

Palavecino, P. (1999) Musculatura asociada al primer y segundo arco visceral de algunos anuros leptodactílidos. *Cuadernos de Herpetología*, 13, 37–46.

Pisanó, A. (1954/1957) Factores de especialización endócrino-sexual en anfibios de alta montaña y de otras regiones del noroeste argentino. *Anales del Departamento de Investigación Científica (DIC), Universidad Nacional de Cuyo*, 2, 1–28.

Pisanó, A. & Rengel, D. (1954) Enanismo en larvas de *Telmatobius hauthali schreiteri* de las altas montañas del oeste argentino. *Scientia Genetica*, 4, 227–271.

Rohlf, F.J. & Bookstein, F.L. (1990) *Proceedings of the Michigan Morphometrics Workshop*, University of Michigan Museum of Zoology, Special publication No. 2, 380 pp.

Sinsch, U., Hein, K. & Glum, B. (2005) Reassessment of central Peruvian Telmatobiinae (genera *Batrachophrynus* and *Telmatobius*): osteology, palmar morphology and skin histology. *Monografías de Herpetología*, 7, 239–260.

Trueb L. 1979. Leptodactylid frogs of the genus *Telmatobius* in Ecuador, with the description of a new species. *Copeia*, 1979, 714–733.

Vellard, J. (1946) El género *Telmatobius* en la República Argentina. *Acta Zoologica Lilloana*, 3, 313–326.

Vellard, J. (1960) Estudios sobre batracios andinos. VI. Notas complementarias sobre *Telmatobius*. *Memorias del Museo de Historia Natural Javier Prado*, 10, 1–19.

Vera Candioti, M.F. (2007) Anatomy of anuran tadpoles from lentic water bodies: systematic relevance and correlation with feeding habits. *Zootaxa*, 1600, 1–175.

Vera Candioti, M.F., Brusquetti, F. & Netto, F. (2007) Morphological characterization of *Leptodactylus elenae* tadpoles (Anura: Leptodactylidae: *L. fuscus* group), from central Paraguay. *Zootaxa*, 1435, 1–17.

Wassersug, R.J. (1976a) A procedure for differential staining of cartilage and bone in whole formaline fixed vertebrates. *Stain Technology*, 51, 131–134.

Wassersug, R.J. (1976b) Oral morphology of anuran larvae: terminology and general description. *Occasional Papers of the Museum of Natural History, University of Kansas*, 48, 1–23.

Wassersug, R.J. & Heyer, W.R. (1988) A survey of internal oral features of leptodactyloid larvae (Amphibia: Anura). *Smithsonian Contributions to Zoology*, 457, 1–99.

Wassersug, R.J. & Hoff, K. (1979) A comparative study of the buccal pumping mechanism of tadpoles. *Biological Journal of the Linnean Society*, 12, 225–259.

Wassersug, R.J. & Pyburn, W.F. (1987) The biology of the Pe-ret' toad, *Otophryne robusta* (Microhylidae), with special consideration of its fossorial larva and systematic relationships. *Zoological Journal of the Linnean Society*, 91, 137–169.

Wiens, J.J. (1993) Systematics of the leptodactylid frog genus *Telmatobius* in the Andes of northern Peru. *Occasional Papers Museum Natural History, University of Kansas*, 162, 1–76.

Zelditch, M.L., Swiderski, D.L., Sheets, H.D. & Fink, W.L. (2004) *Geometric Morphometrics for Biologists*, Elsevier Academic Press, 443 pp.